nature COMMUNICATIONS

ARTICLE

Received 3 Jul 2012 | Accepted 26 Nov 2012 | Published 15 Jan 2013

DOI: 10.1038/ncomms2337

High current superconductivity in $FeSe_{0.5}Te_{0.5}$-coated conductors at 30 tesla

Weidong Si[1], Su Jung Han[1], Xiaoya Shi[1], Steven N. Ehrlich[2], J. Jaroszynski[3], Amit Goyal[4] & Qiang Li[1]

Although high-temperature superconductor cuprates have been discovered for more than 25 years, superconductors for high-field application are still based on low-temperature superconductors, such as Nb_3Sn. The high anisotropies, brittle textures and high manufacturing costs limit the applicability of the cuprates. Here we demonstrate that the iron superconductors, without most of the drawbacks of the cuprates, have a superior high-field performance over low-temperature superconductors at 4.2 K. With a CeO_2 buffer, critical current densities $>10^6$ A cm^{-2} were observed in iron-chalcogenide $FeSe_{0.5}Te_{0.5}$ films grown on single-crystalline and coated conductor substrates. These films are capable of carrying critical current densities exceeding 10^5 A cm^{-2} under 30 tesla magnetic fields, which are much higher than those of low-temperature superconductors. High critical current densities, low magnetic field anisotropies and relatively strong grain coupling make iron-chalcogenide-coated conductors particularly attractive for high-field applications at liquid helium temperatures.

[1] Condensed Matter Physics & Materials Science Department, Brookhaven National Laboratory, Upton, New York 11973, USA. [2] National Synchrotron Light Source, Brookhaven National Laboratory, Upton, New York 11973, USA. [3] National High Magnetic Field National Laboratory, Florida State University, 1800 E. Paul Dirac Drive, Tallahassee, Florida 32310, USA. [4] Materials Science and Technology Division, Oak Ridge National Laboratory, Oak Ridge, Tennessee 37831, USA. Correspondence and requests for materials should be addressed to W.S. (email: wds@bnl.gov) or to Q.L. (email: qiangli@bnl.gov).

Iron-based superconductors are semi-metallic materials with transition temperatures, T_c, up to 55 K. The combination of extremely high upper critical fields, $H_{c2}(0)$ (estimated to be on the order of 100 T), moderate H_{c2}^{ab}/H_{c2}^{c} anisotropies (on the order of 1–8) and high irreversibility fields, H_{irr}, makes this class of superconductors particularly appealing for high-field applications[1–8], where the critical current density, J_c, is a major limiting factor. Although the high-T_c cuprates currently hold the records of J_c value among all superconductors, there are quite a few obstacles for their practical application. The extremely high anisotropies up to thousands have made it very difficult to obtain superconducting tapes or wires with their best J_c. The rapid decrease of J_c upon the grain boundary misorientation also made their fabrication much more difficult and complicated. Their brittle textures as well as the high production and raw material costs also hold back their application. Currently, superconductors for high-field application are still based on Nb_3Sn, a low T_c superconductor that allows fields in excess of 20 T to be achieved at 4.2 K. We argue that iron superconductors may be a more competitive candidate to replace these low T_c superconductors for high-field application at liquid helium temperatures.

To achieve this goal, a key task is to find a technique to increase the J_c of iron-superconductor films (or wires) made on practical metal substrates (or inside metal sheath). One of these techniques is to make a proper buffer layer between the superconductor and the substrate. A suitable buffer layer can often prevent undesirable reactions between the superconductor and the substrate, or enhance the superconducting properties of the films and wires. For iron-pnictide films, Tarantini *et al.*[9] recently reported that single-crystalline (La, Sr)(Al, Ta)O_3 substrates with 100 unit cells of epitaxial $SrTiO_3$ (STO) resulted in higher T_c and J_c for Co-doped $BaFe_2As_2$ films. Higher T_c and sharper out-of-plane and in-plane textures of the Fe/$BaFe_2As_2$ bilayers were also realized with 20-nm thick epitaxial Fe buffer layers[10]. A self-field $J_c > 1\,MA\,cm^{-2}$ at 4.2 K has been reported in both Co-doped $BaFe_2As_2$ and SmFeAs(O, F) systems[1,2], as well as in Co-doped $BaFe_2As_2$ thin films on coated conductor substrates[4]. However, the results of high-field performance up close to their H_{irr} at 4.2 K are still missing.

Here we show that epitaxially grown iron-chalcogenide thin films with a CeO_2 buffer layer have a superior high-field performance up to 30 T with $J_c > 1\,MA\,cm^{-2}$ in self-field. Chalcogenides are an interesting sub-class of iron-based superconductors. Even though the T_c of chalcogenides are typically < 20 K, it was found that the T_c of FeSe can reach 37 K under a pressure of ~ 7 GPa (ref. 11). Recently, it was reported that a single-unit cell film of FeSe on a STO substrate may be superconducting > 77 K (ref. 12). They also have the simplest structures among the iron-based superconductors and exhibit lower anisotropies ~ 2, compared with the pnictides, with comparable $H_{c2}(0)$ approaching 50 T (refs 13–15). We have previously reported on the successful growth of $FeSe_{0.5}Te_{0.5}$ (FST) thin films on textured metal templates with biaxially aligned MgO layers, made *via* ion-beam-assisted deposition (IBAD)[3]. These films carry $J_c > 10^4\ A\,cm^{-2}$ under magnetic fields as high as 25 T at about 4 K. However, MgO has a cubic lattice constant of ~ 4.11 Å, which is fairly larger than the in-plane lattice constant of FST, which is around 3.81 Å. CeO_2, a commonly used buffer layer for high-temperature superconductor (HTS) cuprates, has a much closer lattice constant (cubic, $a = 5.41/\sqrt{2} \sim 3.82$ Å) with FST. In this article, we show that CeO_2 buffer can significantly improve the T_c and J_c of FST films both on single-crystalline substrates and coated conductors, such as the rolling-assisted biaxially textured substrate (RABiTS), which have a biaxially textured CeO_2 layer at the top[16]. These films have a self-field J_c as high as $1\,MA\,cm^{-2}$ and maintain a nearly isotropic J_c on the order of $1 \times 10^5\,A\,cm^{-2}$ up to 30 T at 4.2 K.

Results

Structure of FST films on CeO_2-buffered substrates. Figure 1a shows a θ-2θ X-ray diffraction (XRD) scan of a typical FST film grown on a (100) Yttria-stabilized zirconia (YSZ) substrate with a buffer layer of CeO_2. Figure 1b shows the same scan for a film grown on a RABiTS substrate. For both films, only the (00*l*) peaks from the FST film, CeO_2 buffer and substrates are present, indicating that the out-of-plane alignments are good. The CeO_2, YSZ and Y_2O_3 layers, with the NiW base layer, in the RABiTS substrate are clearly seen in the XRD scan. Figure 1c–e shows the

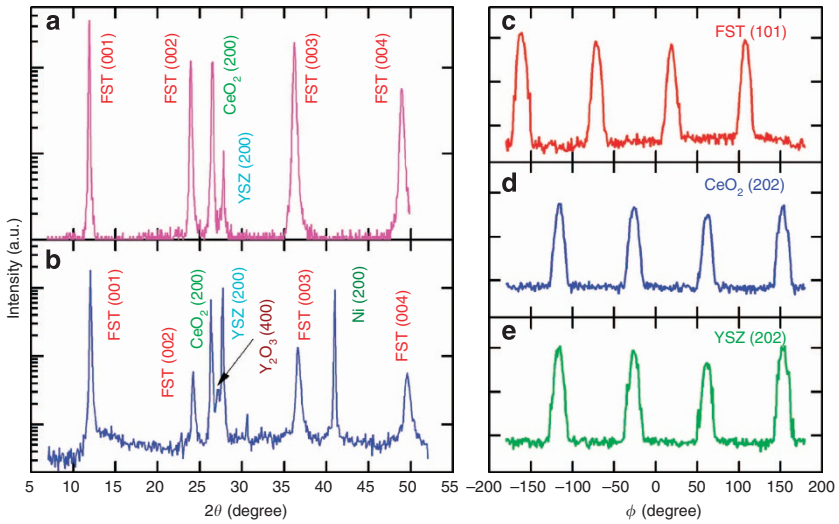

Figure 1 | Structure analysis of FST films by XRD. θ-2θ scan of FST films grown on (**a**) a YSZ single-crystalline substrate with CeO_2 buffer layer and (**b**) a RABiTS substrate. ϕ scan of (**c**) (101) peak from the FST film, (**d**) (202) peak from the CeO_2 buffer layer and (**e**) (202) peak from YSZ buffer layer in a FST film grown on a RABiTS subtrate. Both the film and buffer layers are well aligned in-plane and out-of-plane. The lattice of the FST film is rotated by 45° in the *ab* plane compared with the lattice of CeO_2/YSZ buffer layers.

ϕ scan of the (101) peak from the thin film and the (202) peak from the CeO_2 and YSZ buffer layers in the RABiTS substrate. All of them have four peaks with 90° intervals consistent with four-fold symmetry. Peaks from the thin film and the CeO_2/YSZ buffer layers are separated by 45°, indicating that the lattice of the film is rotated by 45° in the *ab* plane compared with the lattice of CeO_2/YSZ buffer layers and is now aligned cube-on-cube with the NiW substrate. The *c*-axis lattice constant is about 5.90–5.94 Å for both types of films, which is shorter than that of the bulk sample (6.02 Å). This is consistent with our previous results from films grown on other substrates[3,17].

T_c comparison of various FST films and the bulk material. Figure 2 shows the resistive superconducting transitions of various FST thin films and the bulk material. It is clearly seen that FST films (except for that grown on IBAD substrates) have T_c 2–5 K higher than that of bulk. The highest T_c is achieved with a CeO_2 buffer layer, which has an onset T_c >20 K and zero resistance T_c >18 K. The transition width (10–90% normal resistance level) is under 1 K. The most striking finding is that the film grown on RABiTS has a higher T_c than the film grown on single-crystalline substrate without a CeO_2 buffer layer, although the latter actually has a smaller in-plane texture. The full-width half maximum of the (101) peak from the ϕ scan ($\Delta\phi_{101}$) is about 6°, which is smaller than the CeO_2 texture in the RABiTS substrate ($\Delta\phi_{202}\sim7°$). This behaviour was also observed in $Ba(Fe_{1-x}Co_x)_2As_2$ films by Katase *et al.*[4] However, $\Delta\phi_{101}$ for films on single-crystalline substrates without a CeO_2 buffer are just ~2°. Even films on IBAD substrates have better textures ($\Delta\phi_{101}\sim5°$) (ref. 3). These results suggest that the CeO_2 buffer has a much more profound effect on the superconducting properties of FST thin films than the sharpness of the texture in the films themselves. Films on IBAD substrates have the lowest T_c (~11 K) as shown in Fig. 2. This is probably due to its largest lattice mismatch to the FST[3].

J_c of FST films. Figure 3 shows the magnetic field dependence of the J_c of the FST films grown on both CeO_2-buffered single-crystalline YSZ and RABiTS substrates at various temperatures. The J_c of films grown on both substrates are shown to be >1 MA cm^{-2} in self-field at 4.2 K, and remain on the order of 1×10^5 A cm^{-2} up to 31 T—the maximum field we could apply. Notably, the decrease of J_c does not accelerate much at high fields at liquid helium temperatures, which is important for high-field magnet applications. Surprisingly, the J_c of the RABiTS film under higher magnetic fields or at higher temperatures is somehow higher than those of films on single-crystalline substrates, although the film grown on the RABiTS substrate has a macroscopic 6° in-plane misalignment of epitaxial grains, which is much higher than that of the film grown on single-crystalline substrates. It has been well known that a key factor limiting the applications of HTS wires is the high-angle grain boundaries that cause the rapid decrease of J_c. Our X-ray texture analysis indicates an average 7° grain boundary misalignment in the RABiTS substrates we used. It is interesting to note that very high J_c of >3 MA cm^{-2} (77 K, self-field) with well-linked behaviour is routinely obtained for $YBa_2Cu_3O_7$ (YBCO) films on these substrates. This seems to be the case in the FST films. Our observation is markedly different from an earlier report on grain boundaries of $Ba(Fe_{1-x}Co_x)_2As_2$ films, which shows that grain boundaries could significantly reduce the J_c even at low angles[18]. A recent report on films of iron-based superconductors by Katase *et al.*[19] has shown that the critical angle for the rapid J_c decrease is about 9°. This is consistent with our studies, although their films are pnictides, whereas our films are chalcogenides.

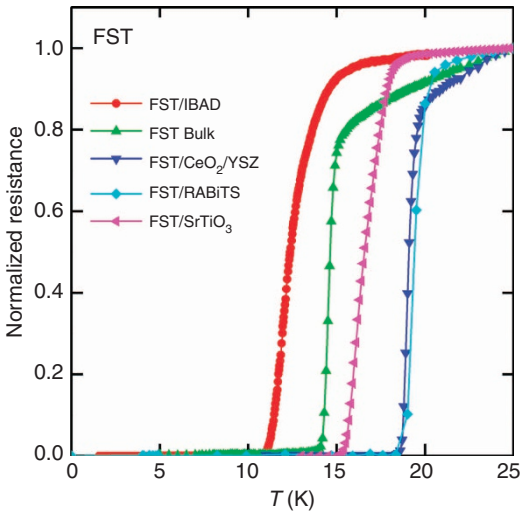

Figure 2 | Resistive superconducting transition of various FST films and the bulk material. T_c of FST films (except for that grown on the IBAD substrate) are 2–5 K higher than that of bulk. Films with CeO_2 buffer layers have the highest T_c with an onset T_c >20 K and zero resistance T_c >18 K.

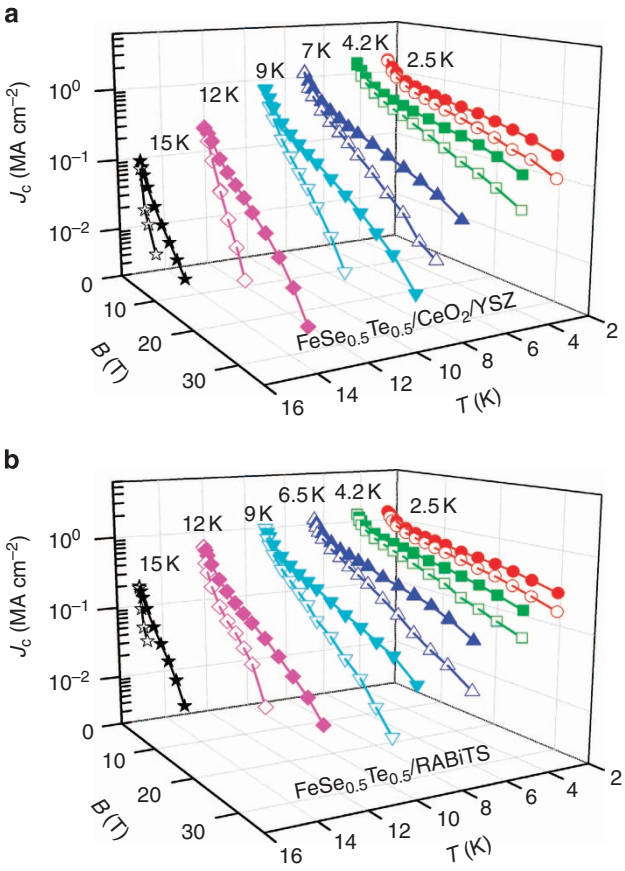

Figure 3 | Critical current densities (J_c) of FST films. J_c of FST films on (**a**) a YSZ substrate with a CeO_2 buffer layer and (**b**) a RABiTS substrate at various temperatures with magnetic field parallel (solid symbols) and perpendicular (open symbols) to the *ab* plane (tape surface). The self-field J_c of both films are above 1 MA cm^{-2} at 4.2 K. Under 30 T of magnetic fields, both films still carry J_c around 1×10^5 A cm^{-2}.

Discussion

In Fig. 4a, we show the field dependence of the volume pinning force F_p for a FST film grown on a RABiTS substrate with the literature data of the second-generation YBCO wire[20,21], thermomechanically processed Nb47Ti alloy[22,23] and small-grain Nb_3Sn wire[24,25]. Clearly, the FST film exhibits superior high-field performance (above ~7 T) over those of other low-temperature superconductors. YBCO and other HTSs currently have higher J_c than the ones typical of iron chalcogenides, but their applications are impeded by high production costs, higher anisotropies, and the rapid decrease of J_c upon grain boundary misorientation. We noted that the cost of the coated conductors mainly depends on the cost of the processing methodologies, not the raw materials. This cost is mostly related to the growth of the thick multiple textured oxide buffer layers, partially to prevent metal template from oxidation, as well as the sophisticated procedures necessary for growing YBCO films near 800 °C and the oxygen annealing afterwards. For the new iron-based coated conductors, the processing temperature is much lower (~400°C) (ref. 17). At this moderate temperature, we expect very limited oxidation of the metal templates, hence thinner and less-complicated buffer structures are likely to produce the same result. Furthermore, oxygen annealing is no longer required. As such, we expect the manufacturing cost of iron-based coated conductors will be reduced, which may make them more attractive on the cost-performance basis.

In Fig. 4b, we show the Kramer's scaling law approximation (solid line), $f_p \sim h^p(1-h)^q$, for a FST film grown on a RABiTS substrate at various temperatures with the field applied both parallel and perpendicular to the tape surface, where $f_p = F_p/F_p^{max}$ is the normalized pinning force density and $h = H/H_{c2}$ is the reduced field. The data for all temperatures and both directions fall approximately on a single line. This appears to suggest that the pinning mechanism is independent of the temperature and field direction. q is found to be equal to 2, which is expected considering that the $(1-h)^2$ term describes the reduction of the superconducting order parameter at high fields[26]. p is found to be ~0.85 ($h^{0.85}$), close to 1. This low-field term indicates that a point-defect core pinning mechanism is at play[26], which is consistent with our previous results of FST films grown on IBAD substrates[3]. In the core pinning regime, F_p is a product of the individual F_p times the pinning centre density. This means that the J_c of FST may still be enhanced by adding more defects to act as pinning centres.

It is not clear what types of defects are responsible for the high J_c values we observed so far, in particular, what is the role of the CeO_2 buffer layer. We attempted to answer these questions by examining the structure properties of our FST films. Our preliminary high-resolution transmission electron microscope study revealed that there might be some intergrowth at the interface between the FST films and the CeO_2 buffer layers. We noted that certain types of intergrowth defects can be effective flux pinning centres in cuprates[27]. Perhaps, they also contribute to the enhanced pinning observed in the FST films on the CeO_2 buffer layers, and result in significantly improved J_c. To understand the flux pinning mechanism, a detailed study of the structure–properties relationship is needed. This is our ongoing effort, and findings will be reported elsewhere.

In conclusion, robust *c*-axis oriented superconducting FST tapes on CeO_2-buffered single-crystalline and RABiTS coated conductor substrates have been made by pulsed-laser deposition. These tapes have a self-field J_c on the order of 1 MA cm^{-2} and carry a nearly isotropic $J_c \sim 10^5$ A cm^{-2} under 30 T at 4.2 K. The CeO_2 buffer layer dramatically improves the superconducting performance of the FST films. It was also found that the low-angle (up to 7°) substrate grain boundary does not depress the J_c of the coated conductor films. These properties show that FST has a very promising future for high-field applications at liquid helium temperatures.

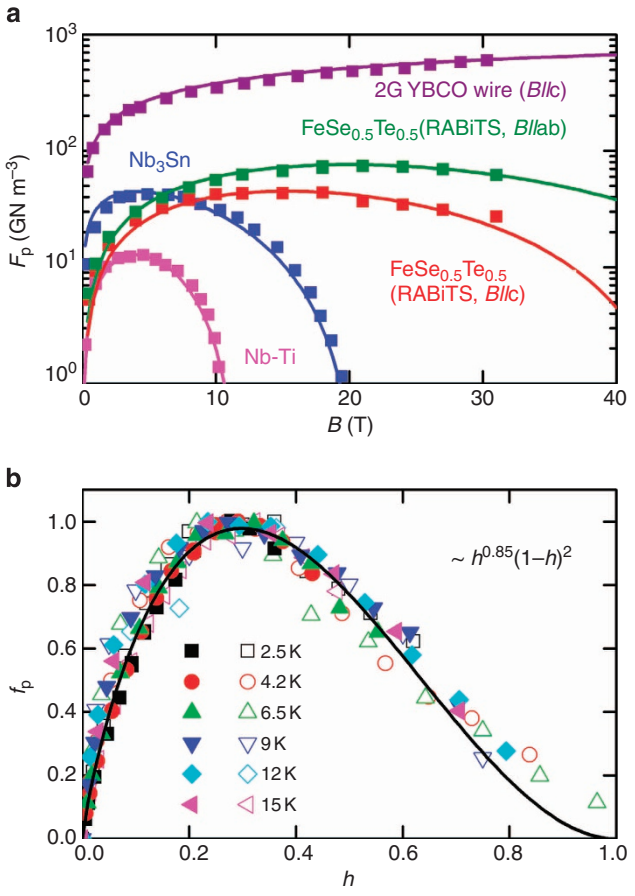

Figure 4 | Pinning force analysis for a FST film grown on RABiTS. (**a**) F_p at 4.2 K of a FST film grown on a RABiTS substrate, compared with the literature data of YBCO 2 G wire[20,21], TCP Nb47Ti[22,23] and Nb_3Sn[24,25]. Solid lines are Kramer's scaling approximations. (**b**) Kramer's scaling of pinning force density f_p versus reduced field h for a FST film grown on a RABiTS substrate at various temperatures with field perpendicular (solid symbols) and parallel (open symbols) to *c*-axis.

Methods

We used pulsed-laser deposition to grow the FST films and CeO_2 buffer layers[17]. Films were deposited on both single-crystalline substrates, such as $LaAlO_3$, STO and YSZ, and RABiTS. RABiTS substrates were originally developed and are presently being used extensively in the production of high-T_c cuprate films. They are comprised of a Ni–W alloy with a series of buffer materials, such as Y_2O_3, YSZ and CeO_2, on top. The topmost is a biaxially textured CeO_2 layer with an in-plane texture of about 7°[16]. Structural characterizations of the various films were performed by XRD at beamline X18A at the National Synchrotron Light Source at Brookhaven National Laboratory. The beam energy is 10 keV. The resistivities and the J_c were measured utilizing a standard four-probe method. Experiments at magnetic fields as high as 31 T were conducted at the National High Magnetic Field Laboratory in Tallahassee, Florida.

References

1. Lee, S. *et al.* Template engineering of Co-doped $BaFe_2As_2$ single-crystal thin films. *Nat. Mater.* **9,** 397–402 (2010).
2. Moll, P. J. W. *et al.* High magnetic-field scales and critical currents in SmFeAs(O, F) crystals. *Nat. Mater.* **9,** 628–633 (2010).
3. Si, W. *et al.* Iron-chalcogenide $FeSe_{0.5}Te_{0.5}$ coated superconducting tapes for high field applications. *Appl. Phys. Lett.* **98,** 262509 (2011).

4. Katase, T. *et al.* Biaxially textured cobalt-doped $BaFe_2As_2$ films with high critical current density over 1MA/cm^2 on MgO-buffered metal-tape flexible substrates. *Appl. Phys. Lett.* **98,** 242510 (2011).
5. Rall, D. *et al.* Critical current densities in ultrathin $Ba(Fe,Co)_2As_2$ microbridges. *Phys. Rev. B* **83,** 134514 (2011).
6. Hunte, F. *et al.* Two-band superconductivity in $LaFeAsO_{0.89}F_{0.11}$ at very high magnetic fields. *Nature* **453,** 903–905 (2008).
7. Jaroszynski, J. *et al.* Upper critical fields and thermally-activated transport of $NdFeAsO_{0.7}F_{0.3}$ single crystal. *Phys. Rev. B* **78,** 174523 (2008).
8. Li, Q., Si, W. & Dimitrov, I. K. Films of iron chalcogenides superconductors. *Rep. Prog. Phys.* **74,** 124510 (2011).
9. Tarantini, C. *et al.* Strong vortex pinning in Co-doped $BaFe_2As_2$ single crystal thin films. *Appl. Phys. Lett* **96,** 142510 (2010).
10. Iida, K. *et al.* Influence of Fe buffer thickness on the crystalline quality and the transport properties of Fe/$Ba(Fe_{1-x}Co_x)_2As_2$ bilayers. *Appl. Phys. Lett.* **97,** 172507 (2010).
11. Margadonna, S. *et al.* Pressure evolution of the low-temperature crystal structure and bonding of the superconductor FeSe ($T_c = 37$ K). *Phys. Rev. B* **80,** 064506 (2009).
12. Wang, Q. Y. *et al.* Interface-induced high-temperature superconductivity in single unit-cell FeSe films on $SrTiO_3$. *Chin. Phys. Lett.* **29,** 037402 (2012).
13. Fang, M. G. *et al.* Weak anisotropy of the superconducting upper critical field in $Fe_{1.11}Te_{0.6}Se_{0.4}$ single crystals. *Phys. Rev. B* **81,** 020509 (2010).
14. Braithwaite, D., Lapertot, G., Knafo, W. & Sheikin, I. Evidence for anisotropic vortex dynamics and pauli limitation in the upper critical field of $FeSe_{1-x}Te_x$. *J. Phys. Soc. Japan* **79,** 053703 (2010).
15. Si, W. *et al.* Superconductivity in epitaxial thin films of $Fe_{1.08}Te{:}O_x$. *Phys. Rev. B* **81,** 092506 (2010).
16. Goyal, A. *Second-Generation HTS Conductors* 29–46 (Kluwer Academic Publishers, 2004; ISBN 1-4020-8117-0).
17. Si, W. *et al.* Enhanced superconducting transition temperature in $FeSe_{0.5}Te_{0.5}$ thin films. *Appl. Phys. Lett.* **95,** 052504 (2009).
18. Lee, S. *et al.* Weak-link behavior of grain boundaries in superconducting $Ba(Fe_{1-x}Co_x)_2As_2$ bicrystals. *Appl. Phys. Lett.* **95,** 212505 (2009).
19. Katase, T. *et al.* Advantageous grain boundaries in iron pnictide superconductors. *Nat. Commun.* **2,** 409 (2011).
20. Xu, A. *et al.* Angular dependence of J_c for YBCO coated conductors at low temperature and very high magnetic fields. *Supercond. Sci. Technol.* **23,** 014003 (2010).
21. Chen., Z. *et al.* A high critical current density MOCVD coated conductor with strong vortex pinning centers suitable for very high field use. *Supercond. Sci. Technol.* **22,** 055013 (2009).
22. Cooley, L. D., Lee, P. J. & Larbalestier, D. C. Flux-pinning mechanism of proximity-coupled planar defects in conventional superconductors: Evidence that magnetic pinning is the dominant pinning mechanism in niobium-titanium alloy. *Phys. Rev. B* **53,** 6638 (1996).
23. Larbalestier, D. C. & West, A. W. New perspectives on flux pinning in niobium-titanium composite superconductors. *Acta Metall.* **32,** 1871–1881 (1984).
24. Godeke, A. A review of the properties of Nb_3Sn and their variation with A15 composition, morphology and strain state. *Supercond. Sci. Technol.* **19,** R68 (2006).
25. Scanlan, R. M., Fietz, W. A. & Koch, E. F. Flux pinning centers in superconducting Nb_3Sn. *J. Appl. Phys.* **46,** 2244–2249 (1975).
26. Ekin, J. W. Unified scaling law for flux pinning in practical superconductors: I. Separability postulate, raw scaling data and parameterization at moderate strains. *Supercond. Sci. Technol.* **23,** 083001 (2010).
27. Yamasaki, H. *et al.* Strong flux pinning due to dislocations associated with stacking faults in $YBa_2Cu_3O_{7-\delta}$ thin films prepared by fluorine-free metal organic deposition. *Supercond. Sci. Technol.* **23,** 105004 (2010).

Acknowledgements

This work was supported by the US Department of Energy, Office of Basic Energy Science, Materials Sciences and Engineering Division, under contract no. DE-AC0298CH10886. RABiTS is a registered trademark of Oak Ridge National Laboratory (ORNL). The RABiTS templates were fabricated at ORNL under funding from the US Department of Energy, Office of Electricity. A portion of this work was performed at the National Synchrotron Light Source (NSLS) and the National High Magnetic Field Laboratory (NHMFL). NSLS is funded by the US Department of Energy. NHMFL is supported by National Science Foundation Cooperative Agreement No. DMR-0654118, the State of Florida and the US Department of Energy.

Author contributions

W.S. and Q.L. designed the study and wrote the manuscript. W.S. made the thin films. W.S., S.J.H. and Q.L. did the low-field measurement. W.S., X.S. and J.J. did the high-field measurement. W.S. and S.N.E. did the XRD experiment. A.G. provided the RABiTS. Q.L. supervised the project. All the authors contributed to discussion on the results for the manuscript.

Additional information

Competing financial interests: The authors declare no competing financial interests.

Reprints and permission information is available online at http://npg.nature.com/reprintsandpermissions/

How to cite this article: Si, W. *et al.* High current superconductivity in $FeSe_{0.5}Te_{0.5}$-coated conductors at 30 tesla. *Nat. Commun.* 4:1347 doi: 10.1038/ncomms2337 (2013).